

A New Mode of Operation of Pd-NHC Systems Studied in a Catalytic Mizoroki–Heck Reaction

Alexander V. Astakhov,[†] Oleg V. Khazipov,[†] Andrey Yu. Chernenko,[†] Dmitry V. Pasyukov,[†] Alexey S. Kashin,[‡] Evgeniy G. Gordeev,[‡] Victor N. Khrustalev,[§] Victor M. Chernyshev,[†] and Valentine P. Ananikov^{*,†,‡,§}

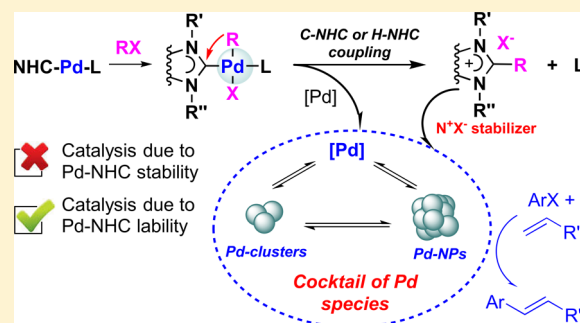
[†]Platov South-Russian State Polytechnic University (NPI), Prosveschenya 132, Novocherkassk 346428, Russia

[‡]Zelinsky Institute of Organic Chemistry, Russian Academy of Sciences, Leninsky Prospekt 47, Moscow 119991, Russia

[§]Peoples' Friendship University of Russia (RUDN University), Miklukho-Maklay St. 6, Moscow 117198, Russia

Supporting Information

ABSTRACT: Metal complexes bearing N-heterocyclic carbene (NHC) ligands are typically considered the system of choice for homogeneous catalysis with well-defined molecular active species due to their stable metal–ligand framework. A detailed study involving 19 different Pd-NHC complexes with imidazolium, benzimidazolium, and triazolium ligands has been carried out in the present work and revealed a new mode of operation of metal-NHC systems. The catalytic activity of the studied Pd-NHC systems is predominantly determined by the cleavage of the metal–NHC bond, while the catalyst performance is strongly affected by the stabilization of in situ formed metal clusters. In the present study, the formation of Pd nanoparticles was observed from a broad range of metal complexes with NHC ligands under standard Mizoroki–Heck reaction conditions. A mechanistic analysis revealed two different pathways to connect Pd-NHC complexes to “cocktail”-type catalysis: (i) reductive elimination from a Pd(II) intermediate and the release of NHC-containing byproducts and (ii) dissociation of NHC ligands from Pd intermediates. Metal-NHC systems are ubiquitously applied in modern organic synthesis and catalysis, while the new mode of operation revealed in the present study guides catalyst design and opens a variety of novel opportunities. As shown by experimental studies and theoretical calculations, metal clusters and nanoparticles can be readily formed from M-NHC complexes after formation of new M–C or M–H bonds followed by C–NHC or H–NHC coupling. Thus, a combination of a classical molecular mode of operation and a novel cocktail-type mode of operation, described in the present study, may be anticipated as an intrinsic feature of M-NHC catalytic systems.



INTRODUCTION

Transition-metal-catalyzed transformations represent a major driving force in the development of the chemical industry and of innovative science in recent decades. Truly notable achievements in ligand design were accomplished with the discovery and the widespread application of N-heterocyclic carbene ligands (NHC ligands). Metal catalysts incorporating NHC ligands (M-NHC) made outstanding contributions to the advancement of cross-coupling reactions, C–H functionalization, the Mizoroki–Heck reaction, metathesis, carbon–heteroatom bond formation, atom-economical transformations, the synthesis of biologically active molecules and pharmaceuticals, the preparation of new advanced materials, and many other areas.¹ The unusual stability of M-NHC complexes (caused by strong metal–ligand binding, shielding by sterically demanding substituents on the carbene ring, and electronic properties) governed the preparation of well-defined molecular catalysts.^{1,2} The highly tunable nature of the NHC ligands facilitated universal practical applications in various areas of organic synthesis and catalysis.^{1–3} As an example of efficient

practical utility, the development of Pd-PEPPSI complexes can be mentioned (PEPPSI = pyridine-enhanced precatalyst preparation, stabilization, and initiation) as readily available, air- and moisture-stable, and easy to handle catalysts.^{1d,n,p,q,4}

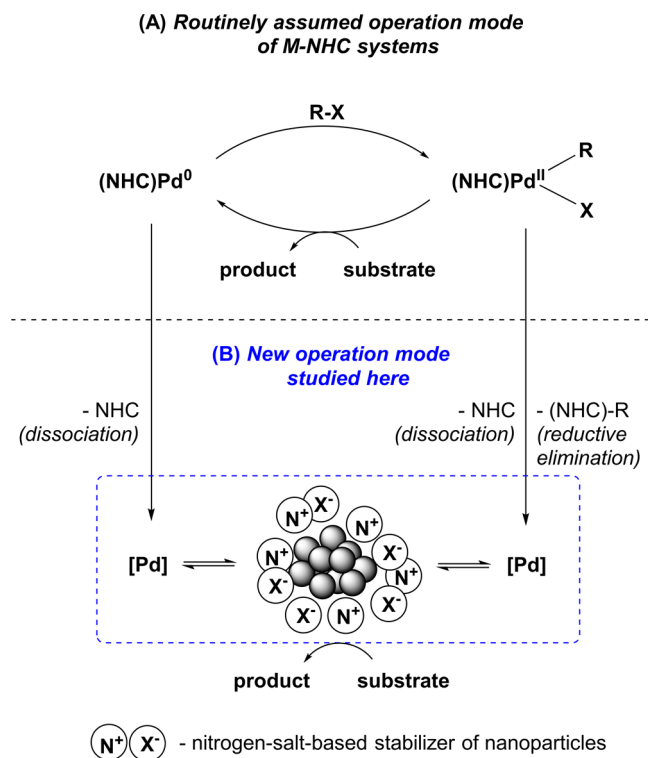
Currently, M-NHC complexes are ubiquitously utilized as catalysts or precursors for homogeneous catalysis with well-defined molecular active species. Nevertheless, despite the great stability attributed to the M-NHC framework, recycling and reuse of M-NHC catalysts remains a demanding challenge, since the complexes are typically of single use in a catalytic transformation.^{1–4} Another approach for designing efficient catalytic systems for fine organic synthesis recently emerged as the concept of a “cocktail” of catalysts.⁵ However, extensive catalyst evolution and in situ transformations were revealed for nanoparticle catalysis and leaching-driven systems,^{5,6} while catalyst dynamics in the case of Pd-NHC systems has only started to emerge.⁷

Received: March 9, 2017



In the present work, we have studied the mechanism of a Pd-NHC catalyzed Mizoroki–Heck reaction utilizing a broad range of metal complexes, and here we describe a new operation mode for these well-known catalysts. Molecular catalysis employing a stable metal–ligand framework (typically assumed for M-NHC catalysts) was found to play only a minor role (Scheme 1A). Catalyst evolution leading to the cleavage of

Scheme 1. Usually Assumed (A) and New (B) Operation Modes for Metal-NHC Catalytic Systems



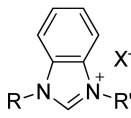
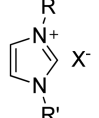
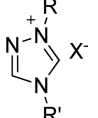
the M–NHC bond and the stabilization of metal nanoparticles with nitrogen quaternary salts were revealed as the processes responsible for catalytic activity in the studied system (Scheme 1B). The nature of the investigated system has shown a drastic difference from the picture routinely assumed for NHC complexes of transition metals.

Although a number of various in situ catalyst transformations and nanoparticle formation reactions were reported for other catalytic systems,^{1–7} a unique mechanistic picture for NHC complexes (including intrinsic reversal stabilization of metal clusters by the released N^+X^- salts) was not addressed in detail for the Heck reaction. Undoubtedly, mechanistic studies of Pd-NHC catalyst evolution during a reaction and the correct determination of the catalytically active species open new, fascinating opportunities in transition-metal catalysis.

RESULTS AND DISCUSSION

Synthesis of the Pd-NHC Complexes. An overview of the NHC ligand precursors used in this study is shown in Table 1. The 1,2,4-triazolium and (benz)imidazolium salts were prepared by the direct alkylation of N-substituted 1,2,4-triazoles, imidazoles, and benzimidazoles.⁸ 1-*tert*-Butyl-1,2,4-triazole was prepared by alkylation of 1,2,4-triazole with *tert*-butyl alcohol in 70% perchloric acid using a procedure for

Table 1. Overview of the Ligand Precursors Used for the Preparation of Pd-PEPPSI Catalysts

	 1a-d	 2a-d	 3a-g
	R	R'	X
1a	^t Bu	^t Bu	Br
1b	Bn	Bn	Cl
1c	Bn	Bn	Br
1d	Me	Me	I
2a	Me	Me	I
2b	Me	^t Bu	Cl
2c	Mes	Mes	Cl
2d	DiPP	DiPP	Cl
3a	Me	Me	I
3b	Me	^t Bu	Br
3c	^t Bu	^t Bu	Br
3d	Bn	Bn	Cl
3e	Bn	Bn	Br
3f	^t Bu	^t Bu	Br
3g	^t Bu	Bn	Br

alkylation of amino- and mercapto-1,2,4-triazoles with *t*-BuOH.⁹

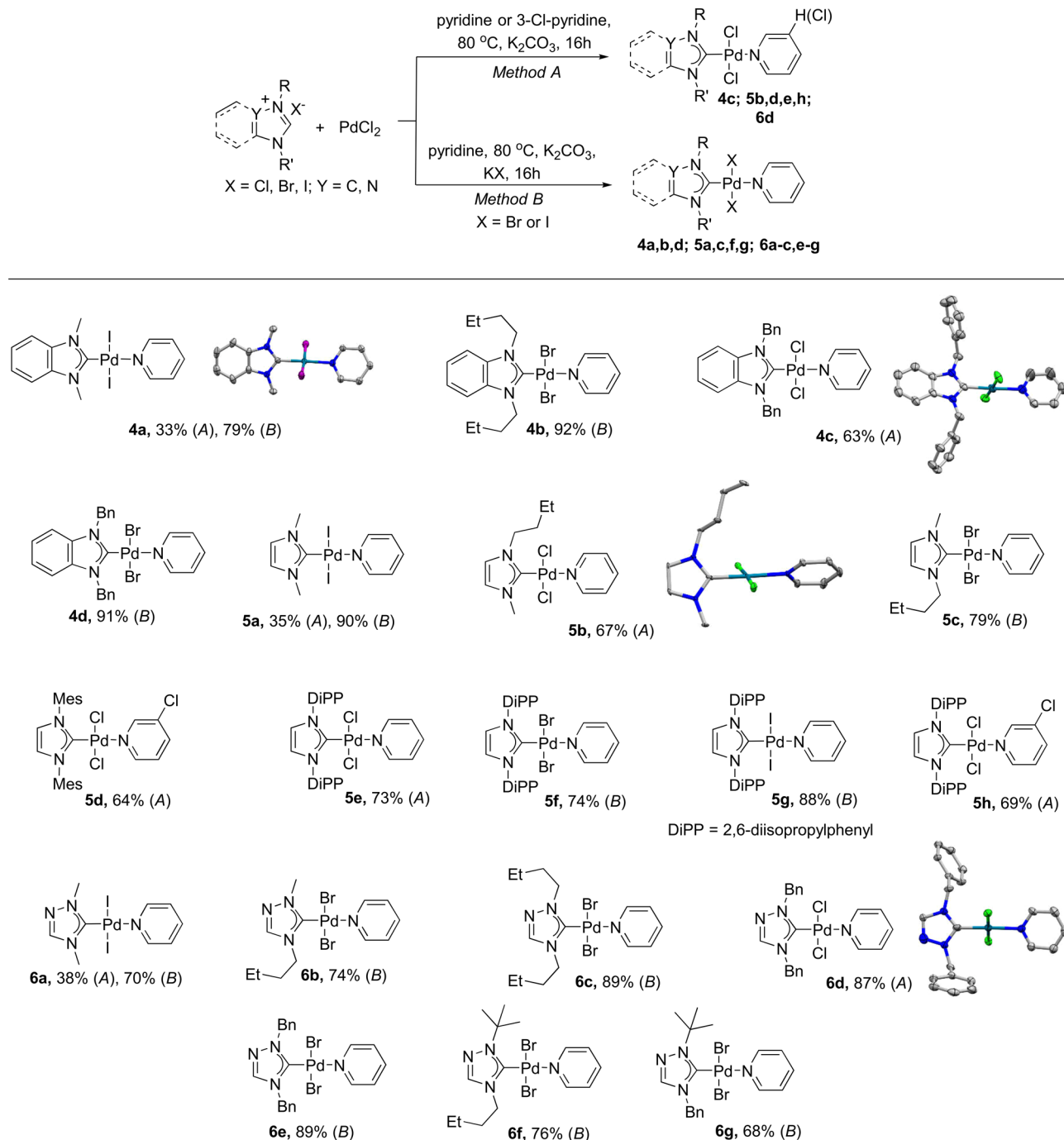
The Pd-NHC complexes 4c, 5b,d,e,h, and 6d were synthesized in 64–87% yields by heating PdCl_2 , K_2CO_3 , and the corresponding pyridine derivative at 80 °C (Scheme 2, method A).^{4a} Dibromo and diiodo Pd-NHC complexes 4a,b,d, 5a,c,f,g, and 6a–c,e–g were synthesized in 67–92% yields using a modified procedure (Scheme 2, method B).^{7d} According to the ^1H and $^{13}\text{C}\{^1\text{H}\}$ NMR spectra, complexes 4–6 were all obtained in the form of *trans* isomers. Specific shifts in the $^{13}\text{C}\{^1\text{H}\}$ NMR resonances at δ 147–164 ppm of metal-bonded C atoms were observed for all of the complexes. The structures of complexes 4a,c, 5b, and 6d were confirmed by single-crystal X-ray diffraction analyses.

Pd-NHC Complexes in a Mizoroki–Heck Reaction. As a representative model system, we have chosen the reactions of iodobenzene (7a) and bromobenzene (7b) with *n*-butyl acrylate (8a) in *N,N*-dimethylformamide (DMF), which is a commonly used solvent. Triethylamine (TEA) and K_2CO_3 were taken as often-used bases, and tetra-*n*-butylammonium bromide (TBAB) was used as an additive. Monitoring of the reaction progress was performed by GC-MS and NMR. In all of the cases, (*E*)-butyl cinnamate (9a) was the only product of the reaction between the compounds 7a,b and 8a.

The catalytic performance of the Pd-NHC complexes 4–6 in the reaction of iodobenzene 7a and acrylate 8a in the presence of TBAB and TEA is presented in Table 2, and the corresponding results for 7b are provided in Tables S2–S4 in the Supporting Information. First, it is necessary to note the common trends observed in the studied system. At 140 °C, most of the complexes revealed high catalytic activity at loadings of 0.005 mol %; however, when the reaction temperature was decreased to 120 and 60 °C, a larger amount of catalyst (0.05 and 0.5 mol %, respectively) was employed to accomplish the reaction within a reasonable time (Table 2).

A comparison of the results obtained for the complexes comprising similar NHC ligands but different halogens (4a,c,d,

Scheme 2. Synthesis of the Pd-NHC Complexes with Various NHC Ligands 4–6



5e,f,g, or **6a,d,e**) showed that the catalytic activity is dependent on the nature of coordinated halogen, changing in the order $I > Br \approx Cl$. Interestingly, the addition of I^- anions to the reaction mixtures catalyzed by the complexes **5e,f** containing Cl^- and Br^- as ligands (Table S1 in the Supporting Information) resulted in a similar enhancement of catalytic activities.

The dependence of the catalytic activity of Pd-NHC complexes **4–6** on the structure of the NHC ligands is more complicated. Thus, variation of the heterocycle class (benzimidazole, imidazole, triazole) has no pronounced effect on the activity (for example, compare the results in the series **4a**, **5a**, **6a**, **4c**, **6d**, **5c**, and **6b**). Bulky N-alkyl groups decrease the catalytic activity at lower temperatures, as observed from

the comparison of the lines for **4b** and **4d**, for **6b** and **6f**, and for **6e** and **6g** at 60 or 120 °C. Interestingly, in the imidazole series complexes **5d–f,h** with bulky N-aryl substituents, Mes and DiPP, containing Cl^- or Br^- as ligands revealed pronouncedly decreased activity; however, complex **5g** ($R = R' = \text{DiPP}$) with iodide ligands demonstrated the highest activity at 60 °C and an average activity at other temperatures in comparison with complexes **4–6**.

It is important to note that the catalytic activities of all the studied Pd-NHC complexes **4–6** did not exceed the catalytic activity of $\text{Pd}(\text{OAc})_2$ and PdCl_2Py_2 , which afforded quantitative yields of **9a** under the same conditions at all studied temperatures (Table 2, entries 20 and 21).

Table 2. Model Mizoroki–Heck Reaction of Iodobenzene (7a) and *n*-butyl Acrylate (8a)^a

Reaction scheme showing the coupling of **7a** (iodobenzene) and **8a** (n-butyl acrylate) to form **9a** (n-butyl cinnamate) using [Pd], TBAB, DMF, TEA, 60-140 °C.

		yield of 9a (%) ^b						
entry	catalyst	[Pd] 0.5 mol %, ^c 60 °C			[Pd] 0.05 mol %, ^c 120 °C		[Pd] 0.005 mol %, ^c 140 °C	
		5 h	10 h	15 h	1 h	5 h	1 h	5 h
1	4a	2	19	83	>99	>99	66	>99
2	4b	0	0	44	6	>99	11	>99
3	4c	0	5	56	23	>99	47	>99
4	4d	0	4	63	61	>99	41	>99
5	5a	0	14	86	>99	>99	78	>99
6	5b	0	9	86	>99	>99	84	>99
7	5c	0	3	70	>99	>99	84	>99
8	5d	0	0	0	5	>99	65	>99
9	5e	0	0	1	4	>99	75	>99
10	5f	0	0	5	12	>99	73	>99
11	5g	30	92	>99	13	>99	62	>99
12	5h	0	0	0	3	>99	69	>99
13	6a	0	9	84	54	>99	52	>99
14	6b	0	5	63	51	>99	53	>99
15	6c	0	2	52	42	>99	60	>99
16	6d	0	2	61	49	>99	41	>99
17	6e	0	3	58	95	>99	56	>99
18	6f	0	0	0	8	>99	66	>99
19	6g	0	1	8	32	>99	59	>99
20	Pd(OAc) ₂	>99	>99	>99	>99	>99	>99	>99
21	PdCl ₂ Pv ₂	>99	>99	>99	>99	>99	>99	>99

^aConditions: 0.5 mmol of PhI, 0.75 mmol of butyl acrylate, 0.5 mmol of TBAB, 1 mmol of TEA, 1 mL of DMF. ^bGC-MS yield of 9a averaged over two runs. ^cPd loadings (mol %) relative to PhI.

Similar trends were observed for the reaction of bromobenzene 7b with acrylate 8a, while acceptable reaction rates were distinguished only at higher temperature (140 °C). The observed catalytic activities of Pd-NHC complexes 4–6 and Pd(OAc)₂ or PdCl₂Py₂ in the presence of TBAB and TEA were comparable (Table S2 in the Supporting Information). Remarkably, the reaction of bromobenzene 7b with acrylate 8a was highly affected by TBAB: in the absence of TBAB only trace levels of product 9a were observed under the same conditions for all of the Pd-NHC catalysts as well as for Pd(OAc)₂ and PdCl₂Py₂ (Table S2). It is noteworthy that the precipitation of palladium black was detected in the experiments without TBAB. It should be mentioned that the addition of TBAB to prevent catalyst deactivation and the precipitation of palladium black is well documented.^{6a,7a,10}

We also tested the catalytic activities of complexes 4–6, Pd(OAc)₂, and PdCl₂Py₂ for reactions between compounds 7a,b and 8a in the presence of TBAB at 140 °C, but using K₂CO₃ as base (Table S3 in the Supporting Information). In comparison with TEA, the reactions proceeded more rapidly, allowing the application of relatively low palladium loadings (0.01 mol %) for both substrates 7a and 7b. Considering statistical averaging, we can propose that the catalytic activity of complexes 4–6 at high temperatures is weakly dependent upon their structures and is very close to that of Pd(OAc)₂ and PdCl₂Py₂. To study a larger substrate scope, we compared the catalytic activity of complex 5h, which is a commercially available and widely applied catalyst, with the activity of Pd(OAc)₂ in the reaction of various bromobenzenes with

different alkenes (Table S4 in the Supporting Information). The activities of 5h and Pd(OAc)₂ were found to be rather similar.

Next, we performed a series of mechanistic studies to reveal the nature of the active species.

Transmission electron microscopy (TEM) of samples of the reaction mixtures after reaction of iodobenzene with acrylate 8a at 60 °C within 5 h revealed the presence of small palladium nanoparticles only in that mixture, where an appreciable yield of product 9a was detected. Thus, small nanoparticles of ~2 nm size were observed in the mixtures with complex 5g (30% yield of 9a) and Pd(OAc)₂ (>99% yield of 9a) (Figure 1).

A mercury test was applied to the reaction of aryl halides 7a,b with acrylate 8a under catalysis with complexes 4a, 5d,g, 6a, and Pd(OAc)₂. No product yields were obtained with any of the catalysts in the temperature range 60–140 °C even after 20 h, when a sufficiently large excess of elemental mercury (Hg(0): [Pd] ≈ 2100:1 mol/mol) was charged to the reaction mixtures at the beginning of the reaction. Applicability of the mercury test for inhibition of Mizoroki–Heck and cross-coupling reactions due to deactivation of Pd nanoparticles is well-known (see, for example refs 6a, 7i,j,q, 10a, and 11).

Important evidence of a key role of the cleavage of metal–NHC bonds on the catalytic process was obtained from comparative kinetics of Pd-NHC and Pd(OAc)₂ catalysis in combination with experiments for successive runs with reloading of the reaction media with fresh substrates. As shown in Figure 2a, in the first reaction run, palladium acetate revealed the highest activity, affording almost quantitative yields

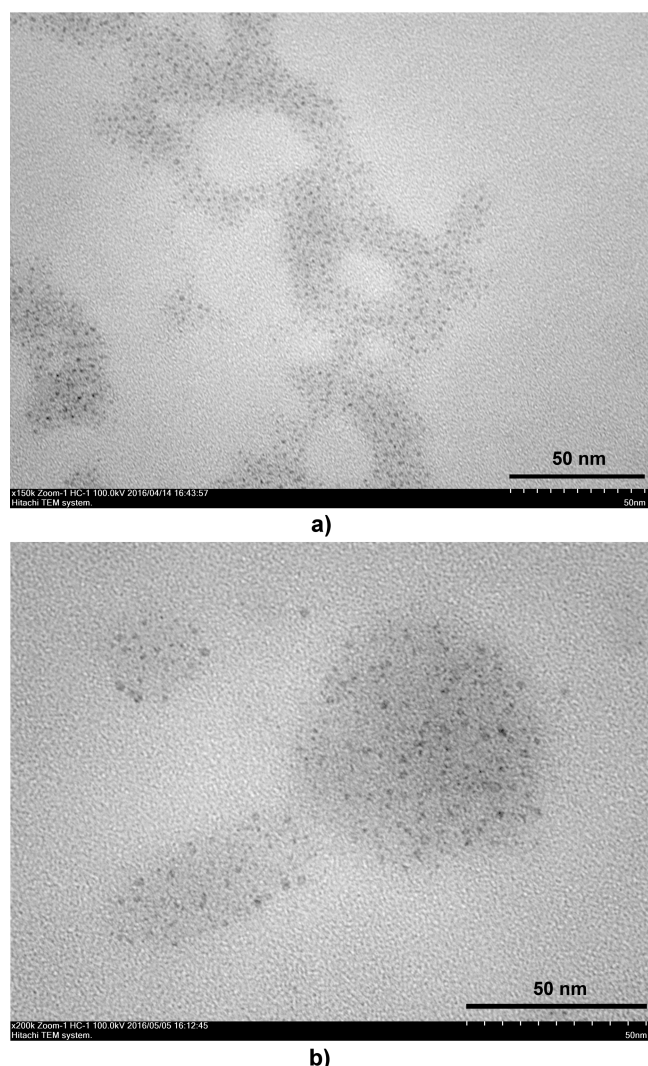


Figure 1. TEM images of palladium nanoparticles isolated from the reaction mixtures after heating 0.5 mmol of **7a**, 0.75 mmol of **8a**, 0.5 mmol of TBAB, and 1 mmol of TEA in 1 mL of DMF: (a) complex **5g** (0.5 mol %) as the catalyst, 60 °C, 5 h; (b) $\text{Pd}(\text{OAc})_2$ (0.5 mol %) as the catalyst, 60 °C, 1 h.

of **9a** within ~40 min. Remarkably, the kinetic curve for precatalyst **5g** demonstrates a sigmoid plot that indicates a significant delay for catalyst activation. Complex **5h** revealed very low activity during the course of the first run. However, for precatalysts **5g,h**, the kinetics changed dramatically after several successive runs. At the fourth run, the observed kinetic curves are almost identical and demonstrate high activity for precatalysts **5g,h** as well as $\text{Pd}(\text{OAc})_2$ (Figure 2b). We also performed similar comparative experiments with reloading runs for all the precatalysts **4–6**, $\text{Pd}(\text{OAc})_2$, and PdCl_2Py_2 at 60 °C (Table S5 in the Supporting Information). Representative examples of successive reaction runs for the precatalysts **6b,f** and $\text{Pd}(\text{OAc})_2$ are shown in Figure 3. As is observed from Figure 3, complex **6f** with a bulky *N-tert*-butyl substituent afforded only a 3% yield of **9a** within the first reaction run, while complex **6b** with an *N*-methyl substituent afforded quantitative yield within the same run.

On the third and successive runs, all of the catalytic systems afforded the same yields of reaction product **9a**. Equal yields (~85%) were measured for the sixth run after 6 h of heating,

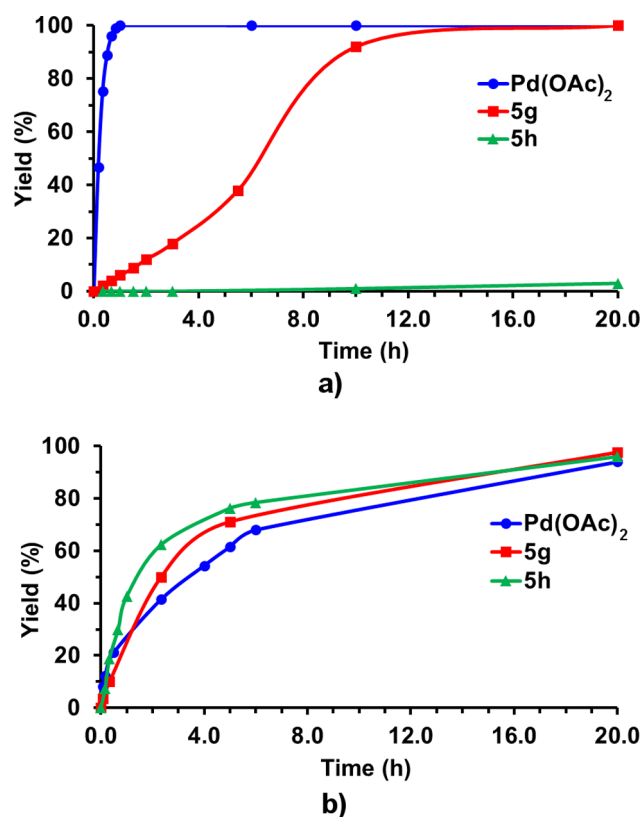


Figure 2. Kinetic curves for the formation of product **9a** in the Mizoroki–Heck reaction between **7a** and **8a** at 60 °C under catalysis with $\text{Pd}(\text{OAc})_2$ (blue lines), complex **5g** (red lines), and complex **5h** (green lines): (a) first run; (b) after three successive reloadings with fresh portions of the substrates **7a** and **8a** (i.e., fourth run). See the Experimental Section and Table S5 in the Supporting Information for details.

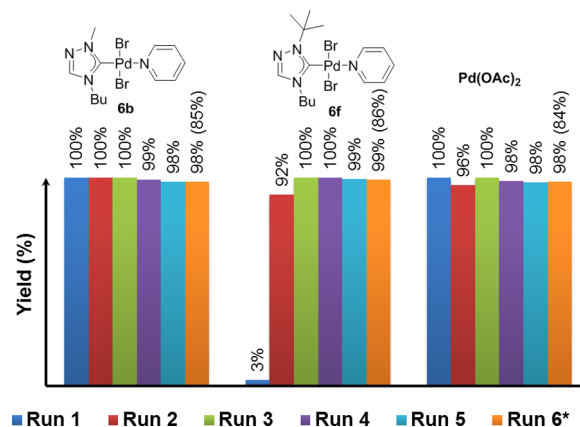


Figure 3. Yields of the product **9a** in the Mizoroki–Heck reaction at 60 °C within 20 h (the yields after 6 h for the sixth run are shown in parentheses) in successive cycles after reloading the reaction media with fresh substrates. See the Experimental Section and Table S5 in the Supporting Information for details.

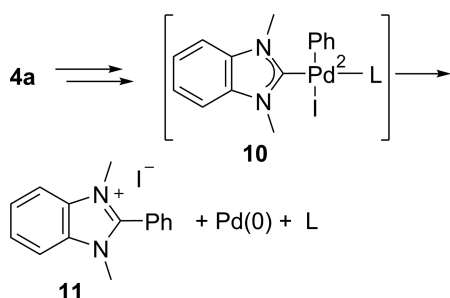
which demonstrated similar kinetic profiles for the studied catalytic systems.

Electron microscopy, a mercury test, kinetic studies, and reloading experiments have undoubtedly highlighted the key role of Pd clusters and “cocktail”-type behavior. These observations are in total agreement with the studies on the

catalytic reactions (Table 2) and prompted us to investigate the process of breaking the Pd–NHC bond.

We attempted to determine the products formed during the degradation of Pd–NHC complexes over the course of the Mizoroki–Heck reaction. A dedicated study of the reaction between compounds **7a** and **8a** was performed with using 1 mol % of catalyst precursor **4a** in the presence of TEA. After separation of Pd black and evaporation of DMF and TEA in vacuo, the organic residue obtained was analyzed by NMR. In addition to product **9a**, new compounds with characteristic signals of a 1,3-dimethylbenzimidazolium fragment were revealed in the residue, while starting complex **4a** was not detected. Subsequent treatment of the residue with Et₂O and water (see the Experimental Section for details) allowed us to obtain compound **11** (5% yield) and initial proligand **1d** (69% yield). Isolation of compounds **11** and **1d** clearly corroborates the degradation of Pd–NHC complexes through the cleavage of the Pd–C_{carbene} bond. Apparently, compound **11** is formed through C–C reductive elimination of the 1,3-dimethyl-2-phenylbenzimidazolium cation from intermediate **10**, which is a product of the oxidative addition of iodobenzene to Pd⁰–NHC (Scheme 3). This assumption was corroborated by heating

Scheme 3. Plausible Pathway of Formation of Compound **11**

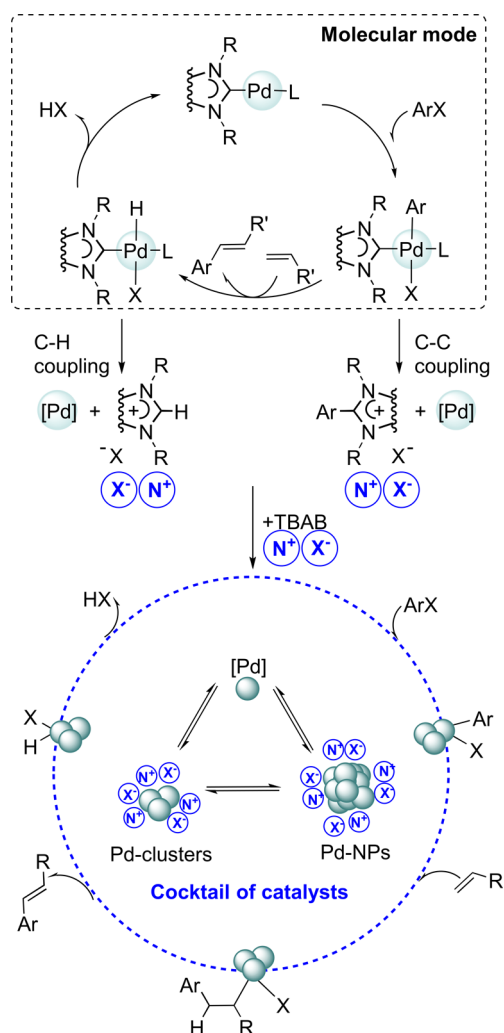


complex **4a** and iodobenzene **7a** under analogous conditions to afford the compound **11** in 50% isolated yield. Such reactivity can be compared with the literature precedents.^{7r,12} Obviously, the reaction affording 2-substituted azolium salts (such as the compound **11**) represents an important pathway of deterioration of NHC ligands and, consequently, the release of “NHC-free” metal species from Pd–NHC catalyst precursors. Analogous cross-coupling reactions of NHC ligands with alkenes or solvent molecules also should not be ruled out.^{12j}

Compound **1d** may also be formed via C–H coupling of the NHC and hydrogen ligands bound to palladium (i.e., the intermediate in the Mizoroki–Heck reaction formed after β -hydrogen elimination; see Scheme 4) or, alternatively, by dissociation of Pd–NHC complexes with subsequent protonation of the released N-heterocyclic carbene. A similar pathway including the dissociation of the Pd–NHC bond and subsequent insertion of the NHC into the C–halogen bond of the aryl halide can also be considered for formation of compound **11**.

To estimate energetic parameters of the proposed C–C reductive elimination pathway, we have carried out theoretical calculations at the PBE1PBE//6-311+G(d)&SDD level including solvent effects at the SMD level (Figure 4). Oxidative addition of Ph–Br to the Pd⁰ complex proceeded via transition state II-TS, which required overcoming an activation barrier of $\Delta G^\ddagger = 25.2$ kcal/mol (I \rightarrow II-TS). The process was found to be energetically favorable with $\Delta G = -25.6$ kcal/mol relative to

Scheme 4. Catalyst Evolution and Nitrogen-Salt-Stabilized “Cocktail”-Type Mode of Mizoroki–Heck Reaction with a Pd–NHC Catalyst Precursor^a



^aTBAB and NHC ligand derived azolium salts may act as N⁺X[−] stabilizers.

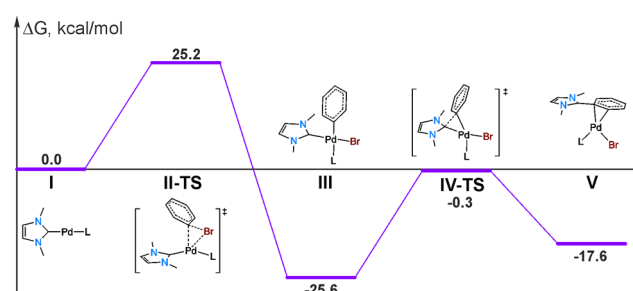


Figure 4. Calculated free energy surface of the C–Br oxidative addition and C–C reductive elimination steps involving the Pd–NHC complex: PBE1PBE//6-311+G(d)&SDD level and solvent effects at SMD level (see the Supporting Information for a model system description and computational details).

initial point I. C–C reductive elimination of the Ph group and NHC ligand proceeded through IV-TS with an activation barrier of $\Delta G^\ddagger = 25.3$ kcal/mol (III \rightarrow IV-TS). The process was also energetically favorable with $\Delta G = -17.6$ kcal/mol relative to initial point I. Thus, C–C coupling involving the

NHC ligand may take place with a similar activation barrier in comparison to the oxidative addition of the substrate. Of course, theoretical calculations on a model system may have some limitations in accuracy. Nevertheless, the computational study clearly confirms the possibility of Pd–NHC bond cleavage, which is in total agreement with experimental findings (Scheme 3).

Theoretical calculations carried out in the present study have shown that dissociation of NHC ligands may also occur, although reductive elimination is the more accessible pathway (see section S4 in the Supporting Information).

It should also be noted that the initial NHC proligands (azolium salts), formed during decomposition of Pd–NHC, can undergo Pd-catalyzed arylation by aryl halides. We have confirmed this possibility in a separate experiment. Heating **1d** and **7a** in DMF in the presence of TEA and Pd(OAc)₂ afforded compound **11** in 40% yield (Scheme S1 in the Supporting Information). Therefore, under the studied catalytic conditions in the presence of a large excess of aryl halide relative to Pd catalyst, the NHC ligands are transformed into 2-arylatedazolium salts (for example, such as compound **11**).

Overall, it is evident that the studied Pd–NHC complexes, **4–6**, decompose during the Mizoroki–Heck reaction through the cleavage of the Pd–C_{carbene} bond to form a mixture of multiple species of palladium, a so-called “cocktail” of catalysts, containing nanoparticles and small metal clusters.

It is important to note that the catalytic performance of the studied systems strongly depended on the stability of the Pd nanoparticles against aggregation to inactive Pd black. Under the harsh reaction conditions (140 °C) used for coupling between bromobenzene **7b** and acrylate **8a**, all of the tested Pd–NHC catalysts precursors were inactive in the absence of TBAB (Pd(OAc)₂ and PdCl₂Py₂ were also inactive). Indeed, the rapid aggregation of palladium nanoparticles and the formation of inactive Pd black did take place without a stabilizer (Table S2 in the Supporting Information). In the presence of a TBAB stabilizer, all of the studied precatalysts have shown high activity (Table S2).

It would be expected that the heterocyclic products (i.e., azolium salts) formed through decomposition of the Pd–NHC complexes can also contribute to stabilization of the palladium nanoparticles. To confirm the possibility of nanoparticle stabilization by azolium salts derived from NHC ligands, we carried out an experiment using compound **2d** instead of TBAB (equimolar amount relative to aryl halide; Table S2 in the Supporting Information). The yield of the cross-coupling product in the presence of **2d** was comparable to the yield in the presence of TBAB. Thus, for the studied reaction, the presence of an equimolar amount (~1 equiv of nitrogen-salt-based stabilizer relative to aryl halide or olefin) is necessary for high performance of the catalytic system.

CONCLUSIONS

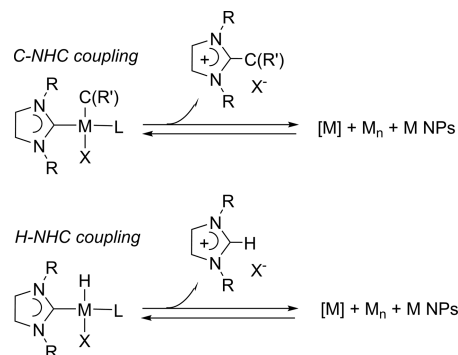
To summarize, in a typical Mizoroki–Heck reaction NHC complexes decomposed through the cleavage of the Pd–C_{carbene} bond and led to the formation of Pd clusters. A mechanism of the chemical transformation of the NHC ligands via C–H or C–C coupling and formation of corresponding azolium salts is proposed here (Scheme 4). Under the studied conditions, a variety of imidazolium, benzimidazolium, and triazolium complexes acted as a source of Pd active species. The stabilizing effect of nitrogen salts prevented agglomeration of the Pd

particles and initiated a catalytic reaction involving a “cocktail”-type catalytic system (Scheme 4).

The new mode of operation of the Pd–NHC complexes described in the present study changes the principles of catalyst design. In the studied reaction, the catalytic activity of the Pd–NHC complexes is defined mainly by their ability to undergo decomposition involving breakage of the metal–ligand framework and the formation of metal clusters or nanoparticles. The ability to form a “cocktail”-type catalytic system depended on the nature of the coordinated halogen and on the type of NHC core. Variation of the heterocycle class revealed a common nature of this transformation, with nanoparticle generation possible for benzimidazole, imidazole, and triazole NHC ligands. Bulky N-alkyl(aryl) groups, in most cases, retarded the decomposition of the complexes, especially at low temperatures. Thus, the substituents at NHC ligands can be varied to affect the rate of release of the Pd species: bulky substituents and strongly bound ligands give rise to “slow-release” catalysts, while small substituents and weakly bound ligands facilitate “fast-release” behavior.

Metal complexes bearing either M–C or M–H bonds are typical intermediates in a number of cross-coupling, C–H functionalization, Heck, and other reactions. The joint experimental and theoretical study carried out in the present article suggests plausible catalyst evolution in such systems leading to generation of NHC-ligand-free metal centers, metal clusters, or nanoparticles (Scheme 5). H–NHC coupling can

Scheme 5. Plausible Catalyst Evolution in M/NHC Systems Involving Intermediate Complexes with M–C and M–H Bonds



be a reversible step, as demonstrated here by the arylation reaction (see above and Scheme S1 in the Supporting Information), and C–NHC coupling can also be a reversible step (Figure 4 and corresponding discussion). This gives rise to dynamic catalytic systems with a possibility of adaptive tuning.¹⁴

Variation of the structure of the Pd–NHC complexes offers a very useful opportunity to regulate the rate of the release of the palladium active species and possibly to control the nature of the stabilizing effect. The findings described in the present study could be of paramount importance for a variety of catalytic systems, as metal–NHC complexes have found widespread applications in modern chemistry. More studies on the subject are anticipated in the near future to evaluate the roles of the molecular mode and the cocktail-type mode of operation within metal–NHC catalytic systems.

EXPERIMENTAL SECTION

General Information. ^1H and $^{13}\text{C}\{^1\text{H}\}$ NMR spectra were recorded on a Bruker DRX 500 instrument at 500 and 125 MHz, respectively, in CDCl_3 . ^1H and $^{13}\text{C}\{^1\text{H}\}$ chemical shifts are given in ppm relative to the residual peak of the solvent (δ 7.26 for CDCl_3) for the proton spectra and the $^{13}\text{C}\{^1\text{H}\}$ CDCl_3 signal (δ 77.16) for the carbon spectra. GC-MS measurements were carried out with an Agilent 7890A GC system, equipped with an Agilent 5975C mass-selective detector (electron impact, 70 eV) and a HP-SMS column (30 m \times 0.25 mm \times 0.25 μm film) using He as carrier gas at a flow of 1.0 mL/min. The following temperature program was used in all GC-MS measurements: initial temperature 40 $^\circ\text{C}$, hold for 3 min, then 25 $^\circ\text{C}$ min $^{-1}$ to 90 $^\circ\text{C}$ and hold for 4 min, then 25 $^\circ\text{C}$ min $^{-1}$ to 190 $^\circ\text{C}$ and hold for 1 min, and then 10 $^\circ\text{C}$ min $^{-1}$ to 260 $^\circ\text{C}$ and hold for 2 min. GC-MS spectra were compared to authentic samples and the NIST mass spectral library to confirm identification. Retention times of compounds were 6.1 min for **8a**, 6.7 min for **7b**, 9.0 min for **7a**, 15.4 min for **9a**, and 17.9 min for dibutyl phthalate (internal standard). High-resolution mass spectra (HRMS) were obtained on a TOF MS instrument using electrospray ionization (ESI) in positive ion mode (interface capillary voltage -4500 V). TEM images were recorded on a Hitachi HT7700 transmission electron microscope (TEM). Elemental analyses were performed using a PerkinElmer 2400 elemental analyzer. Melting points were determined in open capillary tubes in a Thiele apparatus and are uncorrected.

All synthetic manipulations were conducted under an argon or nitrogen atmosphere using standard Schlenk techniques. Dry solvents were used for all manipulations.¹³ DMF was degassed by bubbling argon for 15 min and was stored over activated 3 Å molecular sieves. Column chromatography was conducted on silica gel 60 (230–400 mesh, Merck). Glassware was dried at 120 $^\circ\text{C}$ in an oven for at least 3 h.

1-Butyl-1,2,4-triazole,¹⁵ 1-benzyl-1,2,4-triazole,¹⁵ 1-methylbenzimidazole,¹⁵ 1-butylbenzimidazole,¹⁶ 1,3-dibutyl-1H-benzimidazol-3-ium bromide (**1a**),^{8a} 1,3-dibenzyl-1H-benzimidazol-3-ium chloride (**1b**),¹⁷ 1,3-dimethyl-1H-benzimidazol-3-ium iodide (**1d**),¹⁸ 1,3-dimethyl-1H-imidazol-3-ium iodide (**2a**),^{8a} 1,3-bis(2,4,6-trimethylphenyl)-1H-imidazol-3-ium chloride (**2c**),^{8b} 1,3-bis[2,6-bis(propan-2-yl)phenyl]-1H-imidazol-3-ium chloride (**2d**),^{8b} 1,4-dimethyl-4H-1,2,4-triazol-1-ium iodide (**3a**),^{8a} 1,4-dibutyl-4H-1,2,4-triazol-1-ium bromide (**3c**),^{8a} and 1,4-dibenzyl-4H-1,2,4-triazol-1-ium chloride (**3d**),^{8a} were synthesized as described in the literature. All other chemicals were purchased from Aldrich.

1-tert-Butyl-1H-1,2,4-triazole. A mixture of *tert*-butyl alcohol (1.10 mL, 11.6 mmol), 1,2,4-triazole (0.82 g, 11.9 mmol), and 65% aqueous perchloric acid (5 mL) was stirred at 20 $^\circ\text{C}$ for 3 h and then neutralized with aqueous sodium hydroxide (1 N) to pH 6–7 and extracted with chloroform (3 \times 10 mL). The combined extract was dried with anhydrous sodium sulfate and evaporated to dryness (rotary evaporator). The residue obtained was recrystallized from hexane at -20 $^\circ\text{C}$ to give 1-*tert*-butyl-1,2,4-triazole (1.12 g, 77% yield) as a colorless solid, mp 58–60 $^\circ\text{C}$. ^1H NMR (CDCl_3 , 500 MHz): δ 1.57 (s, 9H, 3CH $_3$), 7.87 (m, 1H, CH of triazole), 8.11 (s, 1H, CH of triazole). $^{13}\text{C}\{^1\text{H}\}$ NMR (CDCl_3 , 125 MHz): δ 29.5, 58.4, 139.8, 151.3. HRMS (ESI): calcd for $\text{C}_6\text{H}_{12}\text{N}_3$ $[\text{M} + \text{H}]^+$ 126.1026, found 126.1030.

General Procedure for the Preparation of 1,4-Dialkyl-1,2,4-triazolium or 1,3-Dialkylbenzimidazolium Halides. A mixture of the corresponding 1-alkyl-1,2,4-triazole or 1-alkylbenzimidazole (0.01 mol), alkyl halide (0.02 mol), and acetonitrile (15 mL) was heated under reflux for 36 h (5 h in the case of MeI or BnBr). Then volatiles were removed in vacuo and the residue obtained was washed with anhydrous diethyl ether (10 mL) and recrystallized from an acetonitrile/acetone mixture (1/10).

1,3-Dibenzyl-1H-benzimidazol-3-ium Bromide (1c). Yield 3.49 g (92%) of colorless crystals, mp 221–223 $^\circ\text{C}$. ^1H NMR (CDCl_3 , 500 MHz): δ 5.87 (s, 4H, 2CH $_2$), 7.34–7.40 (m, 6H, Ar), 7.50–7.52 (m, 6H, Ar), 7.55–7.57 (m, 2H, Ar), 11.82 (s, 1H, H-2). ^1H NMR ($\text{DMSO}-d_6$, 500 MHz): δ 5.86 (s, 4H, 2CH $_2$), 7.35–7.43 (m, 6H, Ar), 7.57–7.62 (m, 6H, Ar), 7.99–8.01 (m, 2H, Ar), 10.55 (s, 1H, H-2).

$^{13}\text{C}\{^1\text{H}\}$ NMR ($\text{DMSO}-d_6$, 125 MHz): δ 49.9, 114.0, 126.7, 128.3, 128.6, 128.9, 131.0, 134.0, 142.9. HRMS (ESI): calcd for $\text{C}_{21}\text{H}_{19}\text{N}_2^+$ $[\text{M} - \text{Br}]^+$ 299.1543, found 299.1542.

4-Butyl-1-methyl-4H-1,2,4-triazol-1-ium Bromide (3b). Yield 2.11 g (96%) of colorless crystals, mp 37–39 $^\circ\text{C}$. ^1H NMR (CDCl_3 , 500 MHz): δ 0.86–0.89 (m, 3H, CH $_3$), 1.29–1.37 (m, 2H, CH $_2$), 1.87–1.93 (m, 2H, CH $_2$), 4.18 (s, 3H, CH $_3$), 4.46–4.49 (m, 2H, CH $_2$), 9.27 (s, 1H, H-3), 11.28 (s, 1H, H-5). $^{13}\text{C}\{^1\text{H}\}$ NMR (CDCl_3 , 125 MHz): δ 13.3, 19.3, 31.9, 39.5, 48.5, 143.0, 144.3. HRMS (ESI): calcd for $\text{C}_7\text{H}_{14}\text{N}_3^+$ $[\text{M} - \text{Br}]^+$ 140.1182, found 140.1186.

1,4-Dibenzyl-4H-1,2,4-triazol-1-ium Bromide (3e). Yield 3.10 g (94%) of colorless crystals, mp 167–169 $^\circ\text{C}$. ^1H NMR (CDCl_3 , 500 MHz): δ 5.61 (s, 2H, CH $_2$), 5.76 (s, 2H, CH $_2$), 7.27–7.30 (m, 6H, Ar), 7.46–7.47 (m, 2H, Ar), 7.59–7.60 (m, 2H, Ar), 9.11 (s, 1H, H-3), 11.76 (s, 1H, H-5). $^{13}\text{C}\{^1\text{H}\}$ NMR (CDCl_3 , 125 MHz): δ 52.0, 56.3, 129.3, 129.4, 129.5, 129.65, 129.67, 129.9, 131.8, 132.1, 142.6, 144.0. HRMS (ESI): calcd for $\text{C}_{16}\text{H}_{16}\text{N}_3^+$ $[\text{M} - \text{Br}]^+$ 250.1339, found 250.1338.

4-Butyl-1-tert-butyl-4H-1,2,4-triazol-1-ium Bromide (3f). Yield 2.41 g (92%) of colorless crystals, mp 199–201 $^\circ\text{C}$. ^1H NMR (CDCl_3 , 500 MHz): δ 0.89–0.92 (m, 3H, CH $_3$), 1.33–1.40 (m, 2H, CH $_2$), 1.68 (s, 9H, CH $_3$), 1.95–2.01 (m, 2H, CH $_2$), 4.59–4.62 (m, 2H, CH $_2$), 9.31 (s, 1H, H-3), 11.55 (s, 1H, H-5). $^{13}\text{C}\{^1\text{H}\}$ NMR (CDCl_3 , 125 MHz): δ 13.5, 19.5, 29.0, 32.3, 48.4, 64.1, 141.1, 144.1. HRMS (ESI): calcd for $\text{C}_{10}\text{H}_{20}\text{N}_3^+$ $[\text{M} - \text{Br}]^+$ 182.1652, found 182.1653.

4-Benzyl-1-tert-butyl-4H-1,2,4-triazol-1-ium Bromide (3g). Yield 2.64 g (89%) of colorless crystals, mp 160–162 $^\circ\text{C}$. ^1H NMR (CDCl_3 , 500 MHz): δ 1.68 (s, 9H, 3CH $_3$), 5.90 (s, 2H, CH $_2$), 7.33–7.34 (m, 3H, Ar), 7.72–7.73 (m, 2H, Ar), 8.95 (s, 1H, H-3), 11.68 (s, 1H, H-5). $^{13}\text{C}\{^1\text{H}\}$ NMR (CDCl_3 , 125 MHz): δ 29.0, 51.6, 64.2, 129.6, 129.7, 129.8, 132.7, 140.9, 143.5. HRMS (ESI): calcd for $\text{C}_{13}\text{H}_{18}\text{N}_3^+$ $[\text{M} - \text{Br}]^+$ 216.1495, found 216.1492.

General Procedure for the Synthesis of Compounds 4–6. **Method A.** The azolium salt **1a,b**, **2b–d**, **3b,d** (0.55 mmol), anhydrous K_2CO_3 (345 mg, 2.5 mmol), and PdCl_2 (89 mg, 0.5 mmol) were charged in a glass tube. Dry pyridine was added (4 mL), the tube was capped with a screw cap, and the mixture was heated with vigorous stirring for 16 h at 80 $^\circ\text{C}$. After it was cooled to 20 $^\circ\text{C}$, the reaction mixture was diluted with CH_2Cl_2 (5 mL) and passed through a short pad of silica gel with CH_2Cl_2 as eluent until the product was completely recovered. The solvent was removed under vacuum (rotary evaporator) at room temperature. The residue that formed was treated with a small volume of hexane (\sim 5 mL); the precipitate that formed was separated by filtration, washed with hexane (5 mL), and dried under vacuum at 20 $^\circ\text{C}$.

Method B. The azolium salt **1a,c,d**, **2a**, **3a–c,e–g** (0.55 mmol), KBr or KI (3.5 mmol), anhydrous K_2CO_3 (345 mg, 2.5 mmol), and PdCl_2 (89 mg, 0.5 mmol) were charged in a glass tube. Dry pyridine was added (4 mL), the tube was capped with a screw cap, and the mixture was heated with vigorous stirring for 16 h at 80 $^\circ\text{C}$. After it was cooled to room temperature, the reaction mixture was diluted with CH_2Cl_2 and passed through a short pad of silica gel with CH_2Cl_2 as eluent until the product was completely recovered. The solvent was removed under vacuum (rotary evaporator) at room temperature. The residue obtained was treated with a small volume of hexane (\sim 5 mL); the precipitate that formed was separated by filtration, washed with hexane (5 mL), and dried under vacuum at 20 $^\circ\text{C}$.

(1,3-Dimethyl-1,3-dihydro-2H-benzimidazol-2-ylidene)diiodo-(pyridine)palladium (4a). Yield 0.096 g (33%, method A), 0.231 g (79%, method B), yellow prismatic crystals, mp 235–237 $^\circ\text{C}$. ^1H NMR (CDCl_3 , 500 MHz): δ 4.19 (s, 6H, 2CH $_3$), 7.27–7.31 (m, 2H, Ar), 7.34–7.39 (m, 4H, Ar), 7.74–7.78 (m, 1H, Ar), 9.09–9.10 (m, 2H, Ar). $^{13}\text{C}\{^1\text{H}\}$ NMR (CDCl_3 , 125 MHz): δ 35.9, 109.9, 123.0, 124.7, 135.3, 137.9, 154.0, 161.5. Anal. Calcd for $\text{C}_{14}\text{H}_{15}\text{I}_2\text{N}_3\text{Pd}$: C, 28.72; H, 2.58; N, 7.18. Found: C, 28.91; H, 2.72; N, 7.01.

Dibromo(1,3-dibutyl-1,3-dihydro-2H-benzimidazol-2-ylidene)-(pyridine)palladium (4b). Yield 0.265 g (92%, method B), yellow prismatic crystals, mp 285–287 $^\circ\text{C}$ dec. ^1H NMR (CDCl_3 , 500 MHz): δ 1.07–1.10 (m, 6H, 2CH $_3$), 1.54–1.62 (m, 4H, 2CH $_2$), 2.20–2.24

(m, 4H, 2CH₂), 4.80–4.84 (m, 4H, 2CH₂), 7.26–7.28 (m, 2H, Ar), 7.36–7.40 (m, 4H, Ar), 7.76–7.80 (m, 1H, Ar), 9.06–9.08 (m, 2H, Ar). ¹³C{¹H} NMR (CDCl₃, 125 MHz): δ 14.0, 20.5, 31.3, 48.8, 110.5, 123.0, 124.7, 134.8, 138.1, 152.7, 161.6. Anal. Calcd for C₂₀H₂₇Br₂N₃Pd: C, 41.73; H, 4.73; N, 7.30. Found: C, 41.39; H, 4.56; N, 7.51.

Dichloro(1,3-dibenzyl-1,3-dihydro-2H-benzimidazol-2-ylidene)-(pyridine)palladium (4c). Yield 0.175 g (63%, method A), yellow prismatic crystals, mp 268–270 °C dec. ¹H NMR (CDCl₃, 500 MHz): δ 6.27 (s, 4H, 2CH₂), 7.06–7.12 (m, 4H, 2CH₂), 7.31–7.39 (m, 8H, Ar), 7.61–7.63 (m, 4H, Ar), 7.75–7.78 (m, 1H, Ar), 8.99–9.00 (m, 2H, Ar). ¹³C{¹H} NMR (CDCl₃, 125 MHz): δ 53.3, 111.6, 123.4, 124.7, 128.1, 128.4, 129.1, 134.7, 135.2, 138.3, 151.4, 164.9. Anal. Calcd for C₂₆H₂₃Cl₂N₃Pd: C, 56.29; H, 4.18; N, 7.57. Found: C, 56.26; H, 4.36; N, 7.28.

Dibromo(1,3-dibenzyl-1,3-dihydro-2H-benzimidazol-2-ylidene)-(pyridine)palladium (4d). Yield 0.288 g (91%, method B), yellow prismatic crystals, mp 285–287 °C dec. The physical and spectral characteristics of the product obtained are identical with those described in the literature.¹⁹

(1,3-Dimethyl-1,3-dihydro-2H-imidazol-2-ylidene)diiodo-(pyridine)palladium (5a). Yield 0.095 g (35%, method A), 0.242 g (90%, method B), yellow prismatic crystals. The physical and spectral characteristics of the product obtained are identical with those described in the literature.²⁰

(1-Butyl-3-methyl-1,3-dihydro-2H-imidazol-2-ylidene)dichloro-(pyridine)palladium (5b). Yield 0.132 g (67%, method A), yellow prismatic crystals, mp 118–120 °C. ¹H NMR (CDCl₃, 500 MHz): δ 1.02 (t, J = 7.5 Hz, 3H, CH₃), 1.44–1.52 (m, 2H, CH₂), 2.03–2.08 (m, 2H, CH₂), 4.15 (s, 3H, CH₃), 4.54 (t, J = 7.4 Hz, 2H, CH₂), 6.89–6.90 (m, 2H, 2CH of imidazole), 7.33–7.36 (m, 2H, Ar), 7.74–7.78 (m, 1H, Ar), 8.98–9.00 (m, 2H, Ar). ¹³C{¹H} NMR (CDCl₃, 125 MHz): δ 13.9, 20.0, 32.8, 38.1, 50.8, 121.7, 123.0, 124.6, 138.1, 148.7, 151.4. Anal. Calcd for C₁₃H₁₉Cl₂N₃Pd: C, 39.57; H, 4.85; N, 10.65. Found: C, 39.29; H, 5.01; N, 10.38.

Dibromo(1-butyl-3-methyl-1,3-dihydro-2H-imidazol-2-ylidene)-(pyridine)palladium (5c). Yield 0.191 g (79%, method B), yellow prismatic crystals, mp 135–137 °C. ¹H NMR (CDCl₃, 500 MHz): δ 1.03 (t, J = 7.5 Hz, 3H, CH₃), 1.46–1.50 (m, 2H, CH₂), 2.05–2.08 (m, 2H, CH₂), 4.09 (s, 3H, CH₃), 4.48–4.51 (m, 2H, CH₂), 6.90–6.91 (m, 2H, 2CH of imidazole), 7.32–7.35 (m, 2H, Ar), 7.73–7.77 (m, 1H, Ar), 9.03–9.05 (m, 2H, Ar). ¹³C{¹H} NMR (CDCl₃, 125 MHz): δ 13.9, 20.1, 32.3, 38.6, 51.1, 121.7, 123.2, 124.6, 137.9, 147.5, 152.7. Anal. Calcd for C₁₃H₁₉Br₂N₃Pd: C, 32.29; H, 3.96; N, 8.69. Found: C, 32.05; H, 4.12; N, 8.45.

[1,3-Bis(2,4,6-trimethylphenyl)-1,3-dihydro-2H-imidazol-2-ylidene]dichloro(3-chloropyridine)palladium (5d). Yield 0.189 g (64%, method A), yellow prismatic crystals. The physical and spectral characteristics of the product obtained are identical with those described in the literature.^{4a}

[1,3-Bis[2,6-bis(propion-2-yl)phenyl]-1,3-dihydro-2H-imidazol-2-ylidene]dichloro(pyridine)palladium (5e). Yield 0.235 g (73%, method A), yellow prismatic crystals. The physical and spectral characteristics of the product obtained are identical with those described in the literature.²¹

[1,3-Bis[2,6-bis(propion-2-yl)phenyl]-1,3-dihydro-2H-imidazol-2-ylidene]dibromo(pyridine)palladium (5f). Yield 0.272 g (74%, method B), yellow prismatic crystals, mp 246 °C dec. ¹H NMR (CDCl₃, 500 MHz): δ 1.12 (d, J = 6.8 Hz, 12H, 4CH₃), 1.50 (d, J = 6.8 Hz, 12H, 4CH₃), 3.25–3.31 (m, 4H, 4CH), 7.06–7.09 (m, 2H, Ar), 7.16 (s, 2H, 2CH of imidazole), 7.36–7.37 (m, 4H, Ar), 7.49–7.53 (m, 3H, Ar), 8.51–8.53 (m, 2H, Ar). ¹³C{¹H} NMR (CDCl₃, 125 MHz): δ 23.6, 26.5, 29.1, 124.16, 124.21, 125.4, 130.4, 135.6, 137.3, 146.8, 152.6, 155.3. Anal. Calcd for C₃₂H₄₁Br₂N₃Pd: C, 52.37; H, 5.63; N, 5.73. Found: C, 52.23; H, 5.60; N, 5.52.

[1,3-Bis[2,6-bis(propion-2-yl)phenyl]-1,3-dihydro-2H-imidazol-2-ylidene]diiodo(pyridine)palladium (5g). Yield 0.363 g (88%, method B), yellow prismatic crystals, mp 210 °C dec. ¹H NMR (CDCl₃, 500 MHz): δ 1.11 (d, J = 6.8 Hz, 12H, 4CH₃), 1.52 (d, J = 6.8 Hz, 12H, 4CH₃), 3.38–3.45 (m, 4H, 4CH), 7.07–7.09 (m, 2H, Ar), 7.21 (s, 2H, 2CH of imidazole), 7.36–7.38 (m, 4H, Ar), 7.50–7.53 (m, 3H, Ar),

8.44–8.45 (m, 2H, Ar). ¹³C{¹H} NMR (CDCl₃, 125 MHz): δ 24.1, 26.6, 29.4, 124.1, 124.5, 125.5, 130.4, 136.4, 137.1, 146.6, 153.5, 156.7. Anal. Calcd for C₃₂H₄₁I₂N₃Pd: C, 46.42; H, 4.99; N, 5.08. Found: C, 46.61; H, 4.78; N, 5.29.

[1,3-Bis[2,6-bis(propion-2-yl)phenyl]-1,3-dihydro-2H-imidazol-2-ylidene]dichloro(3-chloropyridine)palladium (5h). Yield 0.235 g (69%, method A), yellow prismatic crystals, mp 238–240 °C (lit. mp 240 °C).^{4a} The physical and spectral characteristics of the product obtained are identical with those described in the literature.^{4a}

(2,4-Dimethyl-2,4-dihydro-3H-1,2,4-triazol-3-ylidene)diiodo-(pyridine)palladium (6a). Yield 0.102 g (38%, method A), 0.188 g (70%, method B), yellow prismatic crystals, mp 163–165 °C. ¹H NMR (CDCl₃, 500 MHz): δ 4.00 (s, 3H, CH₃), 4.16 (s, 3H, CH₃), 7.34–7.37 (m, 2H, Ar), 7.75–7.78 (m, 1H, Ar), 7.94 (s, 1H, CH of triazole), 9.02–9.03 (m, 2H, Ar). ¹³C{¹H} NMR (CDCl₃, 125 MHz): δ 36.4, 40.9, 124.8, 138.0, 143.3, 153.2, 154.0. Anal. Calcd for C₉H₁₂I₂N₄Pd: C, 20.15; H, 2.25; N, 10.44. Found: C, 20.25; H, 2.50; N, 10.21.

Dibromo(4-butyl-2-methyl-2,4-dihydro-3H-1,2,4-triazol-3-ylidene)(pyridine)palladium (6b). Yield 0.179 g (74%, method B), yellow prismatic crystals, mp 144–146 °C. ¹H NMR (CDCl₃, 500 MHz): δ 1.04 (t, J = 7.5 Hz, 3H, CH₃), 1.44–1.51 (m, 2H, CH₂), 2.12–2.18 (m, 2H, CH₂), 4.28 (s, 3H, CH₃), 4.49–4.52 (m, 2H, CH₂), 7.35–7.37 (m, 2H, Ar), 7.77–7.80 (m, 1H, Ar), 7.93 (s, 1H, CH of triazole), 9.01–9.02 (m, 2H, Ar). ¹³C{¹H} NMR (CDCl₃, 125 MHz): δ 13.8, 19.9, 32.0, 40.6, 49.1, 124.8, 138.2, 142.5, 152.8, 155.1. Anal. Calcd for C₁₂H₁₈Br₂N₄Pd: C, 29.75; H, 3.74; N, 11.56. Found: C, 29.48; H, 3.55; N, 11.84.

Dibromo(2,4-dibutyl-2,4-dihydro-3H-1,2,4-triazol-3-ylidene)-(pyridine)palladium (6c). Yield 0.234 g (89%, method B), yellow prismatic crystals, mp 106–108 °C. ¹H NMR (CDCl₃, 500 MHz): δ 1.01–1.05 (m, 6H, 2CH₃), 1.46–1.52 (m, 4H, CH₂), 2.09–2.17 (m, 4H, 2CH₂), 4.50–4.53 (m, 2H, CH₂), 4.64–4.67 (m, 2H, CH₂), 7.34–7.37 (m, 2H, Ar), 7.76–7.79 (m, 1H, Ar), 7.94 (s, 1H, CH of triazole), 9.01–9.02 (m, 2H, Ar). ¹³C{¹H} NMR (CDCl₃, 125 MHz): δ 13.8, 13.9, 19.96, 20.0, 31.4, 31.9, 49.2, 53.2, 124.8, 138.2, 142.4, 152.8, 154.4. Anal. Calcd for C₁₅H₂₄Br₂N₄Pd: C, 34.21; H, 4.59; N, 10.64. Found: C, 34.42; H, 4.85; N, 10.69.

Dichloro(2,4-dibenzyl-2,4-dihydro-3H-1,2,4-triazol-3-ylidene)-(pyridine)palladium (6d). Yield 0.220 g (87%, method A), yellow prismatic crystals, mp 142–144 °C. ¹H NMR (CDCl₃, 500 MHz): δ 5.85 (s, 2H, CH₂), 5.94 (s, 2H, CH₂), 7.34–7.43 (m, 8H, Ar), 7.51–7.53 (m, 2H, Ar), 7.62–7.64 (m, 2H, Ar), 7.72 (s, 1H, CH of triazole), 7.78–7.81 (m, 1H, Ar), 8.95–8.96 (m, 2H, Ar). ¹³C{¹H} NMR (CDCl₃, 125 MHz): δ 53.1, 56.9, 124.8, 128.7, 128.9, 129.31 (2C), 129.33, 129.5, 133.8, 134.7, 138.5, 142.8, 151.5, 157.1. Anal. Calcd for C₂₁H₂₀Cl₂N₄Pd: C, 49.87; H, 3.99; N, 11.08. Found: C, 49.52; H, 4.02; N, 11.29.

Dibromo(2,4-dibenzyl-2,4-dihydro-3H-1,2,4-triazol-3-ylidene)-(pyridine)palladium (6e). Yield 0.264 g (89%, method B), yellow prismatic crystals, mp 133–135 °C. ¹H NMR (CDCl₃, 500 MHz): δ 5.80 (s, 2H, CH₂), 5.90 (s, 2H, CH₂), 7.34–7.44 (m, 8H, Ar), 7.52–7.53 (m, 2H, Ar), 7.62–7.63 (m, 2H, Ar), 7.70 (s, 1H, CH of triazole), 7.76–7.79 (m, 1H, Ar), 8.98–8.99 (m, 2H, Ar). ¹³C{¹H} NMR (CDCl₃, 125 MHz): δ 53.4, 57.1, 124.8, 128.7, 128.9, 129.3, 129.44, 129.47, 129.52, 133.6, 134.5, 138.2, 142.8, 152.8, 156.5. Anal. Calcd for C₂₁H₂₀Br₂N₄Pd: C, 42.42; H, 3.39; N, 9.42. Found: C, 42.54; H, 3.45; N, 9.62.

Dibromo(4-butyl-2-tert-butyl-2,4-dihydro-3H-1,2,4-triazol-3-ylidene)(pyridine)palladium (6f). Yield 0.200 g (76%, method B), yellow prismatic crystals, mp 99–101 °C. ¹H NMR (CDCl₃, 500 MHz): δ 1.07 (t, J = 7.5 Hz, 3H, CH₃), 1.49–1.57 (m, 2H, CH₂), 2.07 (s, 9H, 3CH₃), 2.13–2.19 (m, 2H, CH₂), 4.69–4.72 (m, 2H, CH₂), 7.33–7.36 (m, 2H, Ar), 7.75–7.78 (m, 1H, Ar), 7.98 (s, 1H, CH of triazole), 8.99–9.00 (m, 2H, Ar). ¹³C{¹H} NMR (CDCl₃, 125 MHz): δ 13.8, 20.1, 31.3, 31.5, 50.2, 62.6, 124.8, 138.1, 141.4, 151.6, 152.9. Anal. Calcd for C₁₅H₂₄Br₂N₄Pd: C, 34.21; H, 4.59; N, 10.64. Found: C, 34.26; H, 4.67; N, 10.35.

(4-Benzyl-2-tert-butyl-2,4-dihydro-3H-1,2,4-triazol-3-ylidene)-dibromo(pyridine)palladium (6g). Yield 0.191 g (68%, method B), yellow prismatic crystals, mp 119–121 °C. ¹H NMR (CDCl₃, 500

MHz): δ 2.08 (s, 9H, 3CH₃), 5.99 (s, 2H, CH₂), 7.34–7.44 (m, 5H, Ar), 7.53–7.55 (m, 2H, Ar), 7.63 (s, 1H, CH of triazole), 7.76–7.79 (m, 1H, Ar), 9.02–9.03 (m, 2H, Ar). ¹³C{¹H} NMR (CDCl₃, 125 MHz): δ 31.3, 54.5, 62.6, 124.8, 129.3, 129.4, 129.8, 133.6, 138.1, 141.2, 152.3, 152.9. Anal. Calcd for C₁₈H₂₂Br₂N₄Pd: C, 38.56; H, 3.96; N, 9.99. Found: C, 38.75; H, 4.05; N, 9.68.

Representative Procedure for the Heck Reaction. Before use, all glassware and materials in contact with the catalytic mixtures were treated with aqua regia to remove any possible palladium residue. Reaction blanks, without added catalyst, were performed to rule out false positives owing to possible contamination by palladium from the reactants. A 7 mL screw-capped glass tube equipped with a magnetic stirring bar was charged with a base (TEA or K₂CO₃, 1 mmol), aryl halide (0.5 mmol), *n*-butyl acrylate (96 mg, 0.75 mmol), and, if necessary, the corresponding tetrabutylammonium salt or compound **2d** (0.5 mmol). A solution of an appropriate amount of Pd catalyst and dibutyl phthalate (14 mg, 0.05 mmol) as an internal standard in DMF (1 mL) was placed in the reaction tube. For the mercury poisoning experiments, the corresponding amount of mercury (Hg(0):[Pd] \approx 2100:1 mol/mol) was added to the reaction mixture before running. The tube was sealed with a screw cap, fitted with a septum, and placed immediately in a thermostated oil bath with vigorous stirring, and that instant was taken as the starting time of the reaction.

For the catalyst reuse experiments, once the reaction time reached an end, the tubes were reloaded at room temperature with a solution of butyl acrylate (64 mg, 0.5 mmol), iodobenzene (102 mg, 0.5 mmol), TEA (51 mg, 0.5 mmol), and dibutyl phthalate (14 mg, 0.05 mmol) in DMF (1 mL). The tubes were then again placed in the oil bath at 60 °C, taking that instant as the new starting time.

Kinetics of the Mizoroki–Heck Reaction. Kinetic experiments were performed in 7 mL glass tubes equipped with a magnetic stirring bar. TEA (101 mg, 1 mmol), TBAB (161 mg, 0.5 mmol), iodobenzene (102 mg, 0.5 mmol), butyl acrylate (96 mg, 0.75 mmol), and dibutyl phthalate (14 mg, 0.05 mmol) were loaded into a reaction tube. Then a solution of Pd catalyst (2.5 μ mol, 0.5 mol %) in DMF (1 mL) was added, and the tube was sealed with a screw cap, fitted with a septum, and placed immediately in a thermostated oil bath with vigorous stirring at 60 °C; that instant was taken as the starting time of the reaction. For the reaction times (data points) indicated in the Figure 2, samples of reaction mixtures (5 μ L) were taken from the tubes, diluted with acetonitrile (1 mL), and then subjected to analysis.

Conversions (%) were determined by GC-MS using dibutyl phthalate as an internal standard, and the corresponding calibration curve was used.

1,3-Dimethyl-2-phenyl-1H-benzimidazol-3-ium Iodide (11). *Method A: Isolation from the Mizoroki–Heck Reaction.* A mixture of TEA (4.04 g, 40 mmol), iodobenzene **7a** (4.08 g, 20 mmol), *n*-butyl acrylate **8a** (3.84 g, 30 mmol), and complex **4a** (0.117 g, 0.2 mmol) in DMF (40 mL) was stirred at 140 °C for 20 h. Then the reaction mixture was filtered through a short pad of Celite from Pd black and the filtrate was concentrated in vacuo by rotary evaporation to give a dark brown oily residue. The residue was treated with Et₂O (3 \times 30 mL) and then extracted with hot water (3 \times 10 mL). The aqueous extract was evaporated in vacuo to a volume of \sim 5 mL and cooled to 10 °C overnight. The precipitate that formed was collected by filtration, recrystallized from water, and dried under vacuum to give 3.5 mg (5% yield) of compound **11** as colorless crystals, mp 272–273 °C (lit. mp 273.5 °C).²² ¹H NMR (DMSO-*d*₆, 500 MHz): δ 3.90 (s, 6H, 2CH₃), 7.76–7.85 (m, 5H, Ar), 7.91–7.93 (m, 2H, Ar), 8.13–8.16 (m, 2H, Ar). ¹³C{¹H} NMR (DMSO-*d*₆, 125 MHz): δ 32.9, 113.4, 121.0, 126.6, 129.5, 130.8, 131.7, 132.9, 150.3. HRMS (ESI): calcd for C₁₅H₁₅N₂⁺ [M-I]⁺ 223.1230, found 223.1234.

The aqueous filtrate was evaporated in vacuo to a small volume (\sim 0.5 mL) and cooled to 10 °C overnight. The precipitate that formed was collected by filtration and dried in vacuo to give 38 mg (69% yield) of compound **1d**.

Method B: Synthesis by the Reaction of Compound 4a, Iodobenzene, and TEA. A mixture of complex **4a** (117 mg, 0.2 mmol), iodobenzene **7a** (408 mg, 2 mmol), TEA (404 mg, 4 mmol), and DMF (4 mL) was stirred at 140 °C for 20 h and then filtered

through a short pad of Celite to remove Pd black. The filtrate was evaporated to dryness in vacuo to give an oily residue. Water (10 mL) was added to the residue and evaporated in vacuo to dryness; the operation was repeated twice to remove residual DMF and TEA. Then the residue was extracted with hot water (3 \times 10 mL), and the extract was evaporated in vacuo to a small volume (\sim 5 mL) and cooled to 10 °C overnight. The precipitate that formed was collected by filtration and dried in vacuo to give 35 mg (50% yield) of compound **11** as colorless crystals.

Method C: Synthesis by the Pd-Catalyzed Reaction of Compound 1d, Iodobenzene, and TEA. A mixture of Pd(OAc)₂ (45 mg, 0.2 mmol), TEA (404 mg, 4 mmol), and DMF (4 mL) was stirred at 140 °C for 30 min. Then compound **1d** (55 mg, 0.2 mmol), iodobenzene **7a** (408 mg, 2 mmol), TEA (404 mg, 4 mmol), and DMF (4 mL) were added to the reaction mixture. The mixture was stirred at 140 °C for 20 h and then filtered through a short pad of Celite to remove Pd black. The filtrate was evaporated to dryness in vacuo to give an oily residue. Water (10 mL) was added to the residue and evaporated in vacuo to dryness; the operation was repeated twice to remove residual DMF and TEA. Then the residue was dissolved in hot water (\sim 5 mL) and the solution was cooled to 10 °C overnight. The precipitate that formed was collected by filtration and dried in vacuo to give 28 mg (40% yield) of compound **11** as colorless crystals.

Electron Microscopy (TEM) Study. For the TEM measurements, a droplet of the analyzed solution (diluted 10 times with pure DMF) was placed on the surface of a carbon-coated copper TEM grid (200 mesh); the solvent was removed under reduced pressure (5–10 mbar) at room temperature, and subsequently the grid was sequentially washed with water (0.5 mL) and isopropyl alcohol (0.5 mL) followed by drying in an air flow. The observations were carried out using a Hitachi HT7700 transmission electron microscope (TEM). Images were acquired in bright-field mode at 100 kV accelerating voltage.

X-ray Crystal Structure Determination of Compounds 4a,c, 5b, and 6d. X-ray diffraction data were collected on the “Belok” beamline of the National Research Center “Kurchatov Institute” (Moscow, Russian Federation) using a Rayonix SX165 CCD detector. All images were collected using an oscillation range of 1.0° and corrected for absorption using the Scala program.²³ The data were indexed, integrated, and scaled using the utility iMOSFLM in the CCP4 program.²⁴ For details, see the Supporting Information. The structures were determined by direct methods and refined by full-matrix least-squares techniques on *F*² with anisotropic displacement parameters for non-hydrogen atoms. All hydrogen atoms were placed in calculated positions and refined within the riding model with fixed isotropic displacement parameters (*U*_{iso}(H) = 1.5*U*_{eq}(C) for the CH₃ groups and *U*_{iso}(H) = 1.2*U*_{eq}(C) for the other groups). All calculations were carried out using the SHELXTL program.²⁵ Crystallographic data for **4a,c**, **5b**, and **6d** have been deposited with the Cambridge Crystallographic Data Center. CCDC 1515061 (**4a**), CCDC 1515062 (**4c**), CCDC 1515063 (**5b**), and CCDC 1515064 (**6d**) contain supplementary crystallographic data for this paper. These data can be obtained free of charge from the Director, CCDC, 12 Union Road, Cambridge CB2 1EZ, U.K. (fax, + 44 1223 336033; e-mail, deposit@ccdc.cam.ac.uk; web, www.ccdc.cam.ac.uk).

■ ASSOCIATED CONTENT

Supporting Information

The Supporting Information is available free of charge on the ACS Publications website at DOI: 10.1021/acs.organomet.7b00184.

Additional experimental data, NMR spectra, HRMS data, details of the X-ray structure determinations, and a detailed description of theoretical calculations (PDF) Optimized Cartesian coordinates with the self-consistent-field energies (at the PBE1PBE/6-311+G(d)&SDD level) (XYZ)

Crystallographic data for **4a** (CIF)

Crystallographic data for **4c** (CIF)

Crystallographic data for **5b** (CIF)

Crystallographic data for **6d** (CIF)

AUTHOR INFORMATION

Corresponding Author

* E-mail: val@ioc.ac.ru.

ORCID

Valentine P. Ananikov: 0000-0002-6447-557X

Notes

The authors declare no competing financial interest.

ACKNOWLEDGMENTS

Synthetic part was financially supported by the Russian Science Foundation (RSF grant 14-23-00078), and mechanistic studies were supported by RSF grant 14-50-00126. The authors also thank the Shared Research Center “Nanotechnologies” of the Platov South-Russian State Polytechnic University and the Department of Structural Studies of Zelinsky Institute of Organic Chemistry for analytical services and P. V. Dorovatovskii and Y. V. Zubavichus (National Research Center “Kurchatov institute”, Moscow, Russia) for their help in collection and treatment of the synchrotron experimental data. X-ray studies were supported by the Ministry of Education and Science of the Russian Federation (Agreement number 02.a03.21.0008). Catalyst decomposition studies were supported by Russian Foundation for Basic Research (RFBR grant 16-29-10786).

REFERENCES

- (1) Selected representative examples among many others: (a) Herrmann, W. A. *Angew. Chem., Int. Ed.* **2002**, *41*, 1290–1309. (b) Littke, A. F.; Fu, G. C. *Angew. Chem., Int. Ed.* **2002**, *41*, 4176–4211. (c) Fürstner, A. *Angew. Chem., Int. Ed.* **2000**, *39*, 3012–3043. (d) Hopkinson, M. N.; Richter, C.; Schedler, M.; Glorius, F. *Nature* **2014**, *510*, 485–496. (e) Díez-González, S.; Marion, N.; Nolan, S. P. *Chem. Rev.* **2009**, *109*, 3612–3676. (f) Beletskaya, I. P.; Cheprakov, A. V. *Chem. Rev.* **2000**, *100*, 3009–3066. (g) Vougioukalakis, G. C.; Grubbs, R. H. *Chem. Rev.* **2010**, *110*, 1746–1787. (h) Samojłowicz, C.; Bieniek, M.; Grela, K. *Chem. Rev.* **2009**, *109*, 3708–3742. (i) Lin, J. C. Y.; Huang, R. T. W.; Lee, C. S.; Bhattacharyya, A.; Hwang, W. S.; Lin, I. J. B. *Chem. Rev.* **2009**, *109*, 3561–3598. (j) Dröge, T.; Glorius, F. *Angew. Chem., Int. Ed.* **2010**, *49*, 6940–6952. (k) Kantchev, E. A. B.; O'Brien, C. J.; Organ, M. G. *Angew. Chem., Int. Ed.* **2007**, *46*, 2768–2813. (l) Fortman, G. C.; Nolan, S. P. *Chem. Soc. Rev.* **2011**, *40*, 5151–5169. (m) Würtz, S.; Glorius, F. *Acc. Chem. Res.* **2008**, *41*, 1523–1533. (n) Valente, C.; Çalimsiz, S.; Hoi, K. H.; Mallik, D.; Sayah, M.; Organ, M. G. *Angew. Chem., Int. Ed.* **2012**, *51*, 3314–3332. (o) Wang, F.; Liu, L.-j.; Wang, W.; Li, S.; Shi, M. *Coord. Chem. Rev.* **2012**, *256*, 804–853. (p) Li, H.; Johansson Seechurn, C. C. C.; Colacot, T. J. *ACS Catal.* **2012**, *2*, 1147–1164. (q) Johansson Seechurn, C. C. C.; Kitching, M. O.; Colacot, T. J.; Snieckus, V. *Angew. Chem., Int. Ed.* **2012**, *51*, 5062–5085. (r) Ezugwu, C. I.; Kabir, N. A.; Yusubov, M.; Verpoort, F. *Coord. Chem. Rev.* **2016**, *307*, 188–210. (s) Gildner, P. G.; Colacot, T. J. *Organometallics* **2015**, *34*, 5497–5508.
- (2) A few selected reviews on structure and bonding: (a) Hahn, F. E.; Jahnke, M. C. *Angew. Chem., Int. Ed.* **2008**, *47*, 3122–3172. (b) Díez-González, S.; Nolan, S. P. *Coord. Chem. Rev.* **2007**, *251*, 874–883. (c) Crudden, C. M.; Allen, D. P. *Coord. Chem. Rev.* **2004**, *248*, 2247–2273. (d) Jacobsen, H.; Correa, A.; Poater, A.; Costabile, C.; Cavallo, L. *Coord. Chem. Rev.* **2009**, *253*, 687–703.
- (3) (a) Mahatthananchai, J.; Dumas, A. M.; Bode, J. W. *Angew. Chem., Int. Ed.* **2012**, *51*, 10954–10990. (b) Nelson, D. J. *Eur. J. Inorg. Chem.* **2015**, *2015*, 2012–2027. (c) Nelson, D. J.; Nolan, S. P. *Chem. Soc. Rev.* **2013**, *42*, 6723–6753. (d) Cisnetti, F.; Gibard, C.; Gautier, A. *J. Organomet. Chem.* **2015**, *782*, 22–30. (e) Schmidt, A.; Wiechmann, S.; Otto, C. F. *Adv. Heterocycl. Chem.* **2016**, *119*, 143–172. (f) Ruiz-Castillo, P.; Buchwald, S. L. *Chem. Rev.* **2016**, *116*, 12564–12649.
- (4) (a) O'Brien, C. J.; Kantchev, E. A. B.; Valente, C.; Hadei, N.; Chass, G. A.; Lough, A.; Hopkinson, A. C.; Organ, M. G. *Chem. - Eur. J.* **2006**, *12*, 4743–4748. (b) Organ, M. G.; Chass, G. A.; Fang, D.-C.; Hopkinson, A. C.; Valente, C. *Synthesis* **2008**, *2008*, 2776–2797. (c) Dunsford, J. J.; Cavell, K. J. *Organometallics* **2014**, *33*, 2902–2905. (d) Valente, C.; Pompeo, M.; Sayah, M.; Organ, M. G. *Org. Process Res. Dev.* **2014**, *18*, 180–190. (e) Zeiler, A.; Rudolph, M.; Rominger, F.; Hashmi, A. S. K. *Chem. - Eur. J.* **2015**, *21*, 11065–11071. (f) Price, G. A.; Bogdan, A. R.; Aguirre, A. L.; Iwai, T.; Djuric, S. W.; Organ, M. G. *Catal. Sci. Technol.* **2016**, *6*, 4733–4742. (g) Osińska, M.; Gniewek, A.; Trzeciak, A. M. *J. Mol. Catal. A: Chem.* **2016**, *418–419*, 9–18.
- (5) (a) Kashin, A. S.; Ananikov, V. P. *J. Org. Chem.* **2013**, *78*, 11117–11125. (b) Zaleskiy, S. S.; Sedykh, A. E.; Kashin, A. S.; Ananikov, V. P. *J. Am. Chem. Soc.* **2013**, *135*, 3550–3559. (c) Ananikov, V. P.; Orlov, N. V.; Zaleskiy, S. S.; Beletskaya, I. P.; Khrustalev, V. N.; Morokuma, K.; Musaev, D. G. *J. Am. Chem. Soc.* **2012**, *134*, 6637–6649. (d) Eremin, D. B.; Ananikov, V. P. *Coord. Chem. Rev.* **2017**, DOI: 10.1016/j.ccr.2016.12.021.
- (6) (a) Weck, M.; Jones, C. W. *Inorg. Chem.* **2007**, *46*, 1865–1875. (b) Phan, N. T. S.; Van Der Sluys, M.; Jones, C. W. *Adv. Synth. Catal.* **2006**, *348*, 609–679. (c) Deraedt, C.; Astruc, D. *Acc. Chem. Res.* **2014**, *47*, 494–503. (d) Astruc, D.; Lu, F.; Aranzas, J. R. *Angew. Chem., Int. Ed.* **2005**, *44*, 7852–7872. (e) Ananikov, V. P.; Beletskaya, I. P. *Organometallics* **2012**, *31*, 1595–1604. (f) Balanta, A.; Godard, C.; Claver, C. *Chem. Soc. Rev.* **2011**, *40*, 4973–4985. (g) Trzeciak, A. M.; Ziolkowski, J. J. *Coord. Chem. Rev.* **2005**, *249*, 2308–2322. (h) Trzeciak, A. M.; Ziolkowski, J. J. *Coord. Chem. Rev.* **2007**, *251*, 1281–1293. (i) Hübner, S.; de Vries, J. G.; Farina, V. *Adv. Synth. Catal.* **2016**, *358*, 3–25. (j) Gladysz, J. A. *Chem. Rev.* **2002**, *102*, 3215–3216. (k) Gladysz, J. A. *Pure Appl. Chem.* **2001**, *73*, 1319. (l) Al-Hmoud, L.; Jones, C. W. *J. Catal.* **2013**, *301*, 116–124. (m) Al-Hmoud, L.; Bali, S.; Mahamulkar, S.; Culligan, J.; Jones, C. W. *J. Mol. Catal. A: Chem.* **2014**, *395*, 514–522. (n) Beletskaya, I. P.; Cheprakov, A. V. *Modern Heck Reactions. In New Trends in Cross-Coupling: Theory and Applications; The Royal Society of Chemistry: Cambridge, U.K., 2015; pp 355–478.* (o) Donnelly, K. F.; Petronilho, A.; Albrecht, M. *Chem. Commun.* **2013**, *49*, 1145–1159. (p) Schmidt, A. F.; Kurokhina, A. A.; Larina, E. V. *Catal. Sci. Technol.* **2014**, *4*, 3439–3457. (q) Pla, D.; Gómez, M. *ACS Catal.* **2016**, *6*, 3537–3552. (r) Yasukawa, T.; Miyamura, H.; Kobayashi, S. *ACS Catal.* **2016**, *6*, 7979–7988. (s) Copéret, C.; Chabanas, M.; Petroff Saint-Arroman, R.; Basset, J.-M. *Angew. Chem., Int. Ed.* **2003**, *42*, 156–181. (t) Cantillo, D.; Kappe, C. O. *ChemCatChem* **2014**, *6*, 3286–3305. (u) *Organometallic Chemistry; Fairlamb, I.; Lynam, J., Eds.; The Royal Society of Chemistry: Cambridge, U.K., 2015; Vol. 40.* (v) Fairlamb, I. J. S. *Annu. Rep. Prog. Chem., Sect. B: Org. Chem.* **2006**, *102*, 50–80. (w) Fairlamb, I. J. S.; Lee, A. F. *Fundamental Pd⁰/Pd^{II} Redox Steps in Cross-coupling Reactions: Homogeneous, Hybrid Homogeneous-Heterogeneous to Heterogeneous Mechanistic Pathways for C-C Couplings. In C-H and C-X Bond Functionalization: Transition Metal Mediation; Ribas, X., Ed.; The Royal Society of Chemistry: Cambridge, U.K., 2013; pp 72–107.*
- (7) (a) Muimhneachain, E. O.; McGlacken, G. P., Pd(0) nanoparticles (NPs) as catalysts in cross-coupling reactions and the homogeneous vs. heterogeneous debate. In *Organometallic Chemistry; The Royal Society of Chemistry: Cambridge, U.K., 2016; Vol. 40*, pp 33–53. (b) Azua, A.; Mata, J. A.; Heymes, P.; Peris, E.; Lamaty, F.; Martinez, J.; Colacino, E. *Adv. Synth. Catal.* **2013**, *355*, 1107–1116. (c) Steeples, E.; Kelling, A.; Schilde, U.; Esposito, D. *New J. Chem.* **2016**, *40*, 4922–4930. (d) Martínez-Olíd, F.; Andrés, R.; Flores, J. C.; Gómez-Sal, P. *Eur. J. Inorg. Chem.* **2015**, *2015*, 4076–4087. (e) Ortiz, A. M.; Sánchez-Méndez, A.; de Jesús, E.; Flores, J. C.; Gómez-Sal, P.; Mendicuti, F. *Inorg. Chem.* **2016**, *55*, 1304–1314. (f) Osińska, M.; Gniewek, A.; Trzeciak, A. M. *J. Mol. Catal. A: Chem.* **2016**, *418–419*, 9–18. (g) Shore, G.; Morin, S.; Mallik, D.; Organ, M. G. *Chem. - Eur. J.* **2008**, *14*, 1351–1356. (h) Borja, G.; Monge-Marcet, A.; Pleixats, R.; Parella, T.; Cattoën, X.; Wong Chi Man, M. *Eur. J. Org. Chem.* **2012**, *2012*, 3625–3635. (i) Keske, E. C.; Zenkina, O. V.; Wang, R.

- Crudden, C. M. *Organometallics* **2012**, *31*, 6215–6221. (j) Lin, Y.-C.; Hsueh, H.-H.; Kanne, S.; Chang, L.-K.; Liu, F.-C.; Lin, I. J. B.; Lee, G.-H.; Peng, S.-M. *Organometallics* **2013**, *32*, 3859–3869. (k) Sharma, K. N.; Joshi, H.; Sharma, A. K.; Prakash, O.; Singh, A. K. *Organometallics* **2013**, *32*, 2443–2451. (l) Baier, H.; Metzner, P.; Körzdörfer, T.; Kelling, A.; Holdt, H. J. *Eur. J. Inorg. Chem.* **2014**, *2014*, 2952–2960. (m) Baier, H.; Kelling, A.; Holdt, H. J. *Eur. J. Inorg. Chem.* **2015**, *2015*, 1950–1957. (n) Gürbüz, N.; Karaca, E. O.; Özdemir, I.; Çetinkaya, B. *Turk. J. Chem.* **2015**, *39*, 1115–1157. (o) Maity, R.; Mekic, A.; Van Der Meer, M.; Verma, A.; Sarkar, B. *Chem. Commun.* **2015**, *51*, 15106–15109. (p) Mitsui, T.; Sugihara, M.; Tokoro, Y.; Fukuzawa, S. I. *Tetrahedron* **2015**, *71*, 1509–1514. (q) Baier, H.; Kelling, A.; Schilde, U.; Holdt, H.-J. *Z. Anorg. Allg. Chem.* **2016**, *642*, 140–147. (r) Lefebvre, J. F.; Longevial, J. F.; Molvinger, K.; Clément, S.; Richeter, S. C. R. *Chim.* **2016**, *19*, 94–102. (s) Maity, R.; Verma, A.; Van Der Meer, M.; Hohloch, S.; Sarkar, B. *Eur. J. Inorg. Chem.* **2016**, *2016*, 111–117. (t) Mannathan, S.; Raoufmoghaddam, S.; Reek, J. N. H.; de Vries, J. G.; Minnaard, A. J. *ChemCatChem* **2015**, *7*, 3923–3927. (u) Canseco-Gonzalez, D.; Gniewek, A.; Szulmanowicz, M.; Müller-Bunz, H.; Trzeciak, A. M.; Albrecht, M. *Chem. - Eur. J.* **2012**, *18*, 6055–6062.
- (8) (a) Astakhov, A. V.; Khazipov, O. V.; Degtyareva, E. S.; Khrustalev, V. N.; Chernyshev, V. M.; Ananikov, V. P. *Organometallics* **2015**, *34*, 5759–5766. (b) Hintermann, L. *Beilstein J. Org. Chem.* **2007**, *3*, 22.
- (9) (a) Voitekhovich, S. V.; Lyakhov, A. S.; Ivashkevich, L. S.; Matulis, V. E.; Grigoriev, Y. V.; Gaponik, P. N.; Ivashkevich, O. A. *Tetrahedron* **2012**, *68*, 4962–4966. (b) Chernyshev, V. M.; Vlasova, A. G.; Astakhov, A. V.; Shishkina, S. V.; Shishkin, O. V. *J. Org. Chem.* **2015**, *80*, 375–385.
- (10) (a) Bej, A.; Ghosh, K.; Sarkar, A.; Knight, D. W. *RSC Adv.* **2016**, *6*, 11446–11453. (b) de Vries, J. G. *Dalton Trans.* **2006**, 421–429.
- (11) Sigeev, A. S.; Peregudov, A. S.; Cheprakov, A. V.; Beletskaya, I. P. *Adv. Synth. Catal.* **2015**, *357*, 417–429.
- (12) (a) McGuinness, D. S.; Cavell, K. J.; Skelton, B. W.; White, A. H. *Organometallics* **1999**, *18*, 1596–1605. (b) McGuinness, D. S.; Saendig, N.; Yates, B. F.; Cavell, K. J. *J. Am. Chem. Soc.* **2001**, *123*, 4029–4040. (c) Caddick, S.; Cloke, F. G. N.; Hitchcock, P. B.; Leonard, J.; Lewis, A. K. d. K.; McKerrecher, D.; Titcomb, L. R. *Organometallics* **2002**, *21*, 4318–4319. (d) Campeau, L.-C.; Thansandote, P.; Fagnou, K. *Org. Lett.* **2005**, *7*, 1857–1860. (e) Cavell, K. *Dalton Trans.* **2008**, 6676–6685. (f) Normand, A. T.; Stasch, A.; Ooi, L.-L.; Cavell, K. J. *Organometallics* **2008**, *27*, 6507–6520. (g) Normand, A. T.; Nechaev, M. S.; Cavell, K. J. *Chem. - Eur. J.* **2009**, *15*, 7063–7073. (h) Couzijn, E. P. A.; Zocher, E.; Bach, A.; Chen, P. *Chem. - Eur. J.* **2010**, *16*, 5408–5415. (i) Ghadwal, R. S.; Reichmann, S. O.; Herbst-Irmer, R. *Chem. - Eur. J.* **2015**, *21*, 4247–4251. (j) Lake, B. R. M.; Chapman, M. R.; Willans, C. E., N-Heterocyclic carbenes; partakers not just spectators. In *Organometallic Chemistry*; The Royal Society of Chemistry: Cambridge, U.K., 2016; Vol. 40, pp 107–139.
- (13) Armarego, W. L. F.; Chai, C. L. L. *Purification of Laboratory Chemicals*, 6th ed.; Elsevier: Oxford, U.K., 2009.
- (14) (a) Lehn, J.-M. *Angew. Chem., Int. Ed.* **2015**, *54*, 3276–3289. (b) Lehn, J.-M. *Top. Curr. Chem.* **2011**, *322*, 1–32.
- (15) (a) Astleford, B. A.; Goe, G. L.; Keay, J. G.; Scriven, E. F. V. *J. Org. Chem.* **1989**, *54*, 731–732. (b) Saif, M.; Flower, K. *Transition Met. Chem.* **2013**, *38*, 113–118.
- (16) Gupta, S.; Chatterjee, A.; Das, S.; Basu, B.; Das, B. *J. Chem. Eng. Data* **2013**, *58*, 1–6.
- (17) Starikova, O. V.; Dolgushin, G. V.; Larina, L. I.; Ushakov, P. E.; Komarova, T. N.; Lopyrev, V. A. *Russ. J. Org. Chem.* **2003**, *39*, 1467–1470.
- (18) Rubbiani, R.; Kitanovic, I.; Alborzinia, H.; Can, S.; Kitanovic, A.; Onambele, L. A.; Stefanopoulou, M.; Geldmacher, Y.; Sheldrick, W. S.; Wolber, G.; Prokop, A.; Wölfl, S.; Ott, I. *J. Med. Chem.* **2010**, *53*, 8608–8618.
- (19) Yen, S. K.; Koh, L. L.; Huynh, H. V.; Hor, T. S. A. *Aust. J. Chem.* **2009**, *62*, 1047–1053.
- (20) Khramov, D. M.; Rosen, E. L.; Er, J. A. V.; Vu, P. D.; Lynch, V. M.; Bielawski, C. W. *Tetrahedron* **2008**, *64*, 6853–6862.
- (21) Shi, Y.; Cai, Z.; Peng, Y.; Shi, Z.; Pang, G. *J. Chem. Res.* **2011**, *35*, 161–162.
- (22) Jiang, J.-L.; Shi, Z. *Synth. Commun.* **1998**, *28*, 4137–4142.
- (23) Evans, P. *Acta Crystallogr., Sect. D: Biol. Crystallogr.* **2006**, *62*, 72–82.
- (24) Battye, T. G. G.; Kontogiannis, L.; Johnson, O.; Powell, H. R.; Leslie, A. G. W. *Acta Crystallogr., Sect. D: Biol. Crystallogr.* **2011**, *67*, 271–281.
- (25) Sheldrick, G. M. *Acta Crystallogr., Sect. A: Found. Crystallogr.* **2008**, *64*, 112–122.